Post-print of: Trawka M., Smulko J., Hasse L., Granqvist C., Annanouch F., Ionescu R.: Fluctuation enhanced gas sensing with WO3-based nanoparticle gas sensors modulated by UV light at selected wavelengths. SENSORS AND ACTUATORS B-CHEMICAL.Vol. 234 (2016), pp. 453-461. DOI: 10.1016/j.snb.2016.05.032

Fluctuation enhanced gas sensing with WO_3-based nanoparticle gas sensors modulated by UV light at selected wavelengths

Maciej Trawka[a], Janusz Smulko[a*], Lech Hasse[a], Claes-Göran Granqvist[b], Fatima Ezahra Annanouch[c], Radu Ionescu[c]

[a]Faculty of Electronics, Telecommunications and Informatics, Gdansk University of Technology, Narutowicza 11/12, 80-233 Gdansk, Poland

[b]Department of Engineering Sciences, The Ångström Laboratory, Uppsala University, Sweden

[c]Department of Electronics, Electrical and Automatic Engineering, Rovira i Virgili University, Tarragona, Spain

E-mail: jsmulko@eti.pg.gda.pl

*Author to whom correspondence should be addressed; Tel.: +48-58-348-6095;
Fax: +48-58-348-6095 jsmulko@eti.pg.gda.pl

Abstract: The sensitivity and selectivity of WO_3-based gas sensors can be enhanced by UV-irradiation-induced modulation, especially if different wavelengths are employed. We used fluctuation-enhanced gas sensing, based on measurements of resistance fluctuations in the gas sensor, to study the effects of such modulation on the noise intensity for ambient atmospheres of synthetic air without and with additions of small amounts of ethanol, methane and formaldehyde. Our data confirmed that the method is energy efficient and can be applied to improve gas detection sensitivity and selectivity. The results are strongly dependent on the gaseous species, and a single UV-modulated WO_3-based gas sensor can discriminate between different gases.

Highlights:

- Sensitivity and selectivity of WO_3-based gas sensors can be improved by irradiation with ultraviolet light.
- The wavelength of the UV light is important.
- Fluctuation enhanced gas sensing improves the selectivity of gas detection upon UV irradiation.

Keywords: gas sensor, noise spectroscopy, UV irradiation, sensitivity.

1. Introduction

Metal-oxide-based gas sensors are of much current interest as a consequence of their facile production and simple applications to a wide range of applications. These sensors are promising for the detection of low concentrations of various gases since they are compatible with various fabrication technologies (even nanotechnology) and also because there is a large variety of metal oxides with different gas sensing characteristics [1-3]. Unfortunately, the sensitivity and selectivity of metal-oxide-based sensors are still too low for a number of emerging applications. This problem can be partially solved by using an array of gas sensors with different sensing properties, but this solution is expensive and requires increased amounts of energy for heating because resistive metal-oxide-based gas sensors normally operate at elevated temperature. Consequently, new methods for enhancing the gas detection are a driving force in the field of gas sensing.

Noise spectroscopy, with or without complementary resistance recordings, was proposed more than a decade ago and proved to be a powerful tool for boosting the selectivity and sensitivity of resistive gas sensors [4-6]. The conductivity of these sensors is altered upon exposure to ambient gases and depends on the reducing or oxidizing ability of these gases. The conductivity change depends on the gas concentration, which hence can be monitored. The power spectral density (PSD) of the gas sensors' resistance fluctuations can change concurrently, and these changes can be utilized to provide more efficient gas detection [7-9]. This latter method is referred to as fluctuation-enhanced sensing (FES) [7].

Recently, there have been reports of resistive gas sensors demonstrating a photocatalytic effect when irradiated by ultraviolet (UV) light [10-13]. The pertinent materials (*e.g.*, WO_3 and TiO_2) have been applied to gas sensing for more than two decades [14]. Irradiating sensors of these materials with UV light is an interesting option for activating chemical reactions at the metal oxide surface and could to some extent replace the necessity of running the sensors at high operating temperatures. In the present work we apply UV light of different wavelengths and demonstrate that the FES method then provides even more information about the sensor's ambient atmosphere.

2. Fluctuation enhanced sensing and UV light

Noise at low-frequency f, especially $1/f$ noise, is often employed to assess the quality of materials and devices [15, 16]. Such noise is utilized in the FES method to determine the presence of various gases in the ambient atmosphere where the resistive gas sensors are placed. In the case of WO_3-based gas sensors, the noise sources appear to be similar to those in devices incorporating intrinsic semiconductors [17]. Some common types of noise are thermal noise, shot noise, burst noise, $1/f$ noise and $1/f^2$ noise. The physical origins of these noises are different and are related to the properties of the gas sensitive layer of the

metal oxide and/or the ambient gas. Noise in metal oxides depends strongly on oxygen-related quantities and on the removal of oxygen atoms [18]. Adsorption-desorption of oxygen atoms—and the presence of inhomogeneity, stress, impurities and grain boundaries in the WO_3 layer—causes fluctuations of the oxygen density and thereby fluctuations of the sensor's resistance [19].

In general, the gas sensing process involves of two phenomena: physisorption and chemisorption [20]. Physisorption is a weak adsorption process—usually related to polarization and van der Waals forces between adsorbate and adsorbent—with interaction energies smaller than 1 eV, while chemisorption involves greater covalent forces and partial electron transfer between adsorbent and adsorbate with interaction energies as large as 10 eV. The main noise sources due to the chemical environment are adsorption-desorption of gas molecules, diffusion of the adsorbed molecules on the sensor surface and shot noise of the current flowing through the potential barriers at grain boundaries in the sensing layer. Measured noise spectra involve the superposition of these three noise sources [19, 20]. In metal-oxide gas sensors, gas adsorption–desorption leads to fluctuations of the free-charge density and generates Lorentzian components in the noise spectrum, which then can be characterized by a flat-level amplitude at low frequencies and a higher "corner frequency" signaling the onset of $1/f^2$ dependence. The ensuing $1/f$-like resistance noise spectrum comprises a superposition of such Lorentzians, whose parameters are expected to depend on the ambient gas. When the operating temperature of the sensor, as well as the UV light level, are carefully selected it is possible to observe the corner frequencies of the Lorentzian contributions in the low-frequency noise spectrum, and these data are characteristic for the ambient gas and yield improved gas sensitivity and selectivity. The effect of UV irradiation on gas sensing efficiency was indicated in earlier work by noise measurements on TiO_2 gas sensing layers [21] and also by simply observing changes in DC resistance [22-24].

3. Experimental procedures

Measurements were performed on a prototype WO_3-based nanosensor (see below) irradiated by either of two UV light emitting diodes (LEDs) with different spectral characteristics (Fig. 1). The measurements were performed in the presence of ethanol (C_2H_5OH), methane (CH_4) or formaldehyde (CH_2O) at several concentrations up to a maximum value between 15 and 75 ppm for the various gases. To enable comparisons of the sensors' response at different irradiations, the maximum optical power of the emitted radiation was equal for both diodes; this was accomplished by carefully selecting their DC currents (Fig. 2).

Metal-oxide-based gas sensors usually operate at relatively high temperatures (typically 100–400°C) in order to accelerate chemical reactions between the metal oxide surface and ambient gas molecules. The operating temperature is an important parameter because detection mechanisms are founded on thermo-activated chemical reactions with influence

on sensor performance such as response time, selectivity and power consumption. We set the operating temperature to 200°C, which is convenient for our purposes since UV irradiation is then able to affect the sensors' DC resistance to a significant degree. Consequently, the gas sensor can be effectively modulated by UV light and furthermore requires less heating energy than for most other gas sensing applications.

3.1. WO_3-based gas sensor

Tungsten oxide is an important *n*-type semiconducting material with a band gap of 2.6–2.8 eV and can have advantageous properties for gas sensing, such as a large surface area [25]. The sensor can be significantly improved by decorating its surface with a small amount of noble metals such as Pt or Au [26, 27].

Many techniques can be used to grow WO_3 nanowires (NWs) decorated with metal nanoparticles (NPs), one example being manufacturing based on aerosol-assisted chemical vapour deposition (AACVD) [28-31]. This is a versatile and high-yield technique for growing metal oxides with notable gas sensing properties and was employed to produce the sensor for our present experiments. The synthesis of nanostructures, as well as the decoration with metal nanoparticles and device integration, was realized in a single processing step. AuNP-decorated WO_3-nanowire films were grown at 350°C by AACVD directly onto the electrode area of alumina gas sensor substrates using tungsten hexacarbonyl and hydrogen tetrachloroaurate as precursors. The average size of the AuNPs was 10 nm, while the WO_3-NWs were ~5 μm in length and 60–120 nm in width. Full details on the deposition conditions can be found elsewhere [30]. Figure 1 depicts the AuNP-decorated WO_3-NW gas sensor together with one of the UV diodes employed for irradiation.

3.2. UV diode characteristics

Two different UV-emitting LEDs were used as radiation sources: T5F produced by Seoul Optodevice [32] and denoted LED1, and OSV4YL5451B produced by OptoSupply [33] and denoted LED2. The main parameters of these diodes are given in Table 1 for a DC current of 20 mA. The optical power emitted by these diodes was measured separately in order to determine the operating currents at which the maximum emitted light intensity is the same but lies at different wavelengths (Fig. 2).

The UV light can affect the gas sensor in the following ways [21, 23, 24]: it gives rise to the dissociation of target gas molecules and surface-adsorbed species, and it generates charge carriers and increases the density of free electron–hole pairs. Thus the UV radiation causes an increase of sensor's conductivity, at least in the thin surface layer surface which interacts with the gaseous ambience. The UV irradiation penetrates the gas sensing layer to various depths depending on the wavelength. Thus one expects that different wavelengths of the UV light will induce different effects in the gas sensor. Moreover, the additional energy supplied

by the UV light can reduce the operating temperature of the gas sensing layer and thereby lower the energy consumption in the sensor.

3.3. Measurement setup

The low-frequency noise measurement setup consisted of a specially designed DC current supply unit, a low-noise preamplifier having low equivalent input noise voltage and high input resistance, a hermetic gas chamber with gas flowmeters to control the ambient atmosphere, and a data acquisition board to record voltage fluctuations and DC voltage across the sensor. The carefully shielded input circuit and preamplifier used a self-contained power supply based on batteries, and the sensor was powered by a constant DC current. The data acquisition board (type NI4474) utilized an analog–digital 24-bits converter multiplexed to register signals from two channels, specifically for voltage fluctuations and for DC voltage across the sensor. The frequency bandwidth of the measurement setup could be selected from 0.1 to 10 kHz. Voltage fluctuations were sampled at frequency f_s, given in Table 2, to observe 1/*f*-like noise under different measurement conditions, *i.e*., for selected ambient gas and UV diode. The recorded data samples were further processed—*e.g*., scaled and used to estimate PSDs—by Matlab scripts and built-in functions. The measurement setup was controlled by a computer using LabVIEW software.

4. Results

The sensor was first stabilized in an ambient atmosphere of synthetic air (80% N_2 and 20% O_2, denoted SA), and the flow of a chosen calibration gas was then introduced to obtain a gas mixture of selected concentration. Low and similar flow rates were used for pure SA and for SA with added gases (below 150 ml/min, see Table 2) in order to avoid gas turbulence and allow direct comparisons between consecutive measurements. Changes in the DC resistance R_S were monitored in the presence of the selected calibration gases (75 ppm of C_2H_5OH and 75 ppm of CH_4) and modulated by UV light emitted by the diode LED2 (394 nm). These preliminary results confirmed that the WO_3 gas sensing layer responded to both gases and, moreover, that the response (*e.g*., DC resistance) can be modulated by UV light (Fig. 3). The gas sensor response was repeatable and strongly dependent on the ambient gas; the DC resistance decreased in the presence of C_2H_5OH and increased in the presence of CH_4. The UV irradiation increased the response time of the gas sensor for the various ambient atmospheres. Moreover, UV light irradiation enhanced the relative change of the sensors' DC resistance in the presence of C_2H_5OH and decreased this change when CH_4 was introduced. Additional measurements in an ambient atmosphere of formaldehyde were done using another specimen from the same batch of sensors. We did not observe any significant change of DC resistance upon UV light irradiation, whereas the noise was altered extensively. This result verifies once more the capability of the FES method. Thus we

conclude that UV light can be used to modulate the gas sensing properties of the investigated gas sensing layer, at least for the selected gases and for the present measurement setup.

4.1. Measurements in the presence of ethanol

Detailed gas sensor measurements in the presence of ethanol were performed using the parameters shown in Table 2. The sensor's DC resistance changed upon exposure to ambiences with different C_2H_5OH concentrations, as expected from the previous calibration measurements using LED2 (Fig. 3). The response was different when LED1 (362 nm) was used (Fig. 4); R_S decreased for increased ethanol concentrations but at a different pace than for LED2, which emits at longer wavelengths (394 nm). This difference can be reconciled with variations in the light adsorption: the longer wavelengths penetrate deeper into the WO_3-based gas sensing layer and therefore induce more pronounced changes of its DC resistance despite this light having lower energy than light at shorter wavelengths [34]. The phenomenon is related to changes in adsorption–desorption rates (different for different ambient gases; *cf*. Fig. 3a and Fig. 3b) or to the UV-light-induced decomposition of the gases followed by adsorption–desorption processes related to photocatalytic reactions on the sensor's surface. The effect can be easily utilized to enhance the discrimination between ambient gases or for estimating their concentration. The improvement has to be determined experimentally for the gas of interest and for the selected detection algorithm.

1/*f*-like noise was recorded under the same conditions as those for measuring R_s. The normalized PDS of voltage fluctuations across the sensor, denoted $S(f)$, was estimated and this function was multiplied by frequency and divided by the squared DC bias voltage U_S^2 of the sensor with the object of having a product that exposes the 1/*f*-like noise component and is independent of the sensor's bias conditions [5]. The product $S(f)\cdot f/(U_S)^2$ was obtained at different ethanol concentrations and is presented in Fig. 5. The shapes of the noise spectra are similar: 1/*f*-like noise is apparent in the middle range of the measured frequency bandwidth, sometimes with a clearly visible plateau caused by additive Lorentzian components (generated by adsorption–desorption processes), and thermal noise occurs at high frequencies. The position of the Lorentzian components depends on gas concentration and wavelength of the UV light (Figs. 5b and c). Thus we conclude that the FES method can be applied successfully to detect ethanol using an AuNP-decorated WO_3-NW gas sensing layer and provides detailed information about the gaseous ambience gas as well as improved gas detection.

When LED2 (394 nm) was applied, we observed a strong difference in $S(f)\cdot f/(U_S)^2$ when the ethanol concentration was increased from zero to 25 ppm, whereas only marginal changes were noted at higher concentrations. Thus LED2 is able to improve the gas detection at very low concentrations of ethanol.

4.2. Measurements in the presence of methane

Measurements analogous to the ones above were performed for methane diluted in SA. The DC resistance of the sensor became larger when the gas concentration was increased (Fig. 6) and was dependent on the wavelength of the UV light. The changes of R_S were more intense for LED2, which is characterized by its more long-wavelength radiation. The DC resistance saturated at lower concentrations of methane than of ethanol, and therefore the measurements were limited to 20 ppm of CH_4 and used conditions presented in Table 2. It should be noted that R_S was more erratic in the presence of methane than of ethanol (Fig. 3).

The noise intensities for our selected conditions (Fig. 7) did not change as much as in the case of ethanol. When the measurements were performed without UV light, the spectra were almost independent of methane concentration (Fig. 7a). Introduction of UV light gave rise to changes in the shapes and intensities of the spectra (Figs. 7b and 7c) but only LED2, with longer-wavelength emission, induced spectral changes dependent on methane concentration (Fig. 7c). It should be noted that the product $S(f)\cdot f/(U_S)^2$ went up at increasing methane concentration, which is in contrast with the data observed for ethanol.

4.3. Measurements in the presence of formaldehyde

Additional data were recorded when the sensor was exposed to formaldehyde diluted in SA. The gas sensor was sensitive to this gas via a change of DC resistance and/or noise intensity. However, its DC resistance was almost independent of the UV light (Fig. 8), whereas the product $S(f)\cdot f/(U_S)^2$ was strongly modulated by UV (Fig. 9). Furthermore, low-frequency noise depended on the wavelength of the irradiating light (Figs. 9b and 9c). We can expect further improvements of the formaldehyde detection level for LED2 (394 nm; Fig. 9c) since the noise intensity saturated already at very low gas concentrations. At the latter UV light wavelength, and at frequencies below 5 Hz, the noise intensity was altered very significantly by exposure to as little as little as 5 ppm of CH_2O.

5. Discussion

We found that UV light is able to modulate the DC resistance and resistance noise of sensors based on AuNP-decorated WO_3-NWs, and that this effect depends on the gas and the wavelength of the UV light. The optical power emitted by the UV-LEDs is inversely proportional to the emitted wavelength, and therefore the energy of the photons from the UV diode LED1 (362 nm) is greater than the energy from LED2 (394 nm) (Fig. 2). But the influence of the UV irradiation depends not only on its energy but also on the depth of its penetration inside the irradiated layer, and for assessing the impact of energy on the sensor's DC resistance one should take into account the absorption of the gas medium and

of the sensing layer. Generally, the absorption in the WO_3 sensor layer changes rapidly as a function of the wavelength of the UV light [35]. The absorption in ethanol and methane is weak for the wavelengths of present interest [36], and hence we can claim that the influence of the UV light on the investigated gas sensor is governed by absorption in the sensing layer and may be explained by processes involving surface-oxygen removal [37]. The same conclusion can be suggested for formaldehyde.

Evidently a greater volume of the gas sensing layer being accessible to UV light means a deeper region subjected to oxygen removal and hence to more profound variations of its physical properties. The volume available to UV irradiation depends strongly on the roughness of the sensing layer since the penetration depth of the irradiation was relatively small; the attenuation length of the UV light is only about 150 nm and increases for longer wavelengths [38]. Such a small length, and the volume reachable by UV light, can explain the observed increase of run-in and recovery times when the UV light was applied. Clearly the oxygen molecules from the deeper regions of the gas sensing layer have to diffuse to its surface in order to exhibit an effect of UV irradiation, and this process can take a longer time than the diffusion of the ambient gas inside the gas sensing layer and the replacement of oxygen molecules there. Therefore, additional improvements of the gas sensitivity ought to be easily obtainable by having an optimized morphology of the gas sensing layer which, in its turn, is contingent on the technology for making the layer [39]. The observed effect of a stronger modification of DC resistance or noise level when using UV light with longer wavelengths confirms our reasoning.

The observed Lorentzian-based plateau in the noise spectra, and its shift induced by UV light, are more difficult to reconcile with the arguments above. We may argue that additional energy of the UV light influences adsorption–desorption processes in a way that is analogous to a change of the sensor's operating temperature [1], which means that the result can be different for different gases because of modified reactions between the gas sensing layer and the gaseous ambient.

Our experimental results indicate that the FES method, together with UV light modulation, is more efficient for detecting ethanol than methane, which follows since the relative changes of the DC resistance and noise intensity are more pronounced for ethanol than for methane. Different responses observed for the investigated gases mean that the proposed sensing method is able to improve gas selectivity. We can even assert that combined temperature and UV-light modulation would be able to boost the selectivity and sensitivity even further. The improvement would be observable for the detection or gas concentration prediction by use of regression methods. Further data could lead to enhanced pattern recognition methods when unknown gas mixtures are investigated. Moreover, a combination of UV irradiation and temperature modulation by pulses could limit the energy consumption and presumably decrease the sensors' response times. The specific degree of improvement for selectivity and sensitivity of gas detection depends also on the algorithm for analyzing the data and requires additional and detailed analysis, as presented elsewhere [8].

6. Conclusion

The influence of UV light on AuNP-decorated WO_3-NW gas sensing layers was experimentally investigated by measuring DC resistance and using fluctuation-enhanced sensing. We found that the sensor response is related to photochemical reactions on the surface of the gas sensing material. Thus its properties can be modulated by irradiation, and the observed effect depends critically on the wavelength of the UV light. Such changes were observed both in DC resistance and in resistance noise. Moreover, the power spectral density of the resistance noise changed its slope upon UV irradiation, which provides more information about the ambient gas than the DC resistance alone.

The results of the present work support an endeavor to reduce the number of gas sensors in numerous applications by employing UV light modulation in conjunction with fluctuation-enhanced sensing. The method can readily be implemented by using tiny and relatively cheap UV diodes. This approach leads us to expect better selectivity of gas detection and prediction of gas concentrations than with today's standard techniques. Moreover, we believe that the proposed method can reduce the operating temperature of the gas sensors and therefore contribute to energy-efficient gas detection systems.

Acknowledgements

This research was partially financed by the National Science Center, Poland, project No. UMO-2012/06/M/ST7/00444 "Detection of gases by means of nanotechnological resistance sensors". R.I. acknowledges a 'Ramón y Cajal' fellowship from the Ministry of Economy and Competiveness (MINECO), Spain. C.G.G. received support from the European Research Council under the European Community's Seventh Framework Program (FP/2007–2013)/ERC Grant Agreement No. 267234 ("GRINDOOR"). J.S. was partially financed by the Horizon 2020 Framework Program of the European Community under Grant Agreement no. 645758.

References

1. G. Korotcenkov, Gas response control through structural and chemical modifications of metal oxide films: State of the art and approaches, Sens. Actuators B 107 (2005) 209–232.
2. J. Smulko, J. Ederth, L. Yingfeng, L.B. Kish, M. Kennedy, F. Krus, Gas-sensing by thermoelectric voltage fluctuations in SnO_2 nanoparticle films, Sens. Actuators B 106 (2005) 708–712.

3. P. Heszler, R. Ionescu, E. Llobet, L. F. Reyes, J. Smulko, L.B. Kish, C.G. Granqvist, On the selectivity of nanostructured semiconductor gas sensors, Phys. Status Solidi B 244 (2007) 4331–4335.
4. L.B. Kish, H. Chang, M.D. King, C. Kwan, J.O. Jensen, G. Schmera, J. Smulko, Z. Gingl, C.G Granqvist, Fluctuation-enhanced sensing for biological agent detection and identification, IEEE Trans. Nanotechnol. 10 (2011) 1238–1242.
5. B. Ayhan, C. Kwan, J. Zhou, L.B. Kish, K.D. Benkstein, P.H. Rogers, S. Semancik, Fluctuation enhanced sensing (FES) with a nanostructured, semiconducting metal oxide film for gas detection and classification, Sens. Actuators B 188 (2013) 651–660.
6. J. Ederth, J. Smulko, L. Kish, P. Heszler, C.G. Granqvist, Comparison of classical and fluctuation-enhanced gas sensing with Pd_xWO_3 nanoparticle films, Sens. Actuators B 113 (2005) 310–315.
7. L.B. Kish, R. Vajtai, C.G. Granqvist, Extracting information from noise spectra of chemical sensors: single sensor electronic noses and tongues, Sens. Actuators B 71 (2000) 55–59.
8. Ł. Lentka, J. Smulko, R. Ionescu, R., C.G. Granqvist, L.B. Kish, Determination of gas mixture components using fluctuation enhanced sensing and the LS-SVM regression algorithm. Metrol. Meas. Syst. 22 (2015) 341–350.
9. M. Kotarski, J. Smulko, Hazardous gases detection by fluctuation-enhanced gas sensing, Fluctuations and Noise Lett. 4 (2010) 359–371.
10. Y. Gui, S. Li, J. Xu, C. Li, Study on TiO_2-doped ZnO thick film gas sensors enhanced by UV light at room temperature, Microelectron. J. 39 (2008) 1120–1125.
11. L. Deng, X. Ding, D. Zeng, S. Tian, H. Li, C. Xie, Visible-light activate mesoporous WO_3 sensors with enhanced formaldehyde-sensing property at room temperature, Sens. Actuators B 163 (2012) 260–266.
12. Q. Geng, Z. He, X. Chen, W. Dai, X. Wang, Gas sensing property of ZnO under visible light irradiation at room temperature, Sens. Actuators B 188 (2013) 293–297.
13. M.-H. Chen, C.-S. Lu, R.-J. Wu, Novel $Pt/TiO_2–WO_3$ materials irradiated by visible light used in a photoreductive ozone sensor, J. Taiwan Inst. Chem. Eng. 45 (2014) 1043–1048.
14. M. Radecka, K. Zakrzewska, M. Rękas, $SnO_2–TiO_2$ solid solutions for gas sensors. Sens. Actuators B 47 (1998) 194–204.
15. C.G. Granqvist, S. Green, E.K. Jonson, R. Marsal, G.A. Niklasson, A. Roos, L.B. Kish, Electrochromic foil-based devices: Optical transmittance and modulation range, effect of ultraviolet irradiation, and quality assessment by $1/f$ current noise. Thin Solid Films 516 (2008) 5921–5926.
16. M. Kiwilszo, J. Smulko, Pitting corrosion characterization by electrochemical noise measurements on asymmetric electrodes. J. Solid State Electrochem. 13 (2009) 1681–1686.
17. S. Kogan, Electronic noise and fluctuations in solids. Cambridge University Press, 2008.
18. T. Contraret, T. Florido, J.L. Seguin, K. Aguir, A physics-based noise model for metallic oxide gas sensors characterization, Procedia Eng. 25 (2011) 375–378.

19. S. Gomri, J. Seguin, J. Guerin, K. Aguir, Adsorption–desorption noise in gas sensors: Modelling using Langmuir and Wolkenstein models for adsorption, Sens. Actuators B 114 (2006) 451–459.

20. S. Gomri, J.L. Seguin, J. Guein, K. Aguir, A mobility and free carriers density fluctuations based model of adsorption–desorption noise in gas sensor, J. Phys. D: Appl. Phys. 41 (2008) 065501/1–065501/11.

21. Z. Topalian, J. Smulko, G.A. Niklasson, C.G. Granqvist, Resistance noise in TiO_2-based thin film gas sensors under ultraviolet irradiation, J. Phys. Conf. Ser. 76 (2007) 1–5.

22. T.Y. Yang, H.M. Lin, B.Y. Wei, C.Y. Wu, C.K Lin, UV enhancement of the gas sensing properties of nano-TiO_2, Rev. Adv. Mater. Sci. 4 (2003) 48–54.

23. S. Mishra, C. Ghanshyam, N. Ram, R. P. Bajpai, R. K. Bedi, Detection mechanism of metal oxide gas sensor under UV radiation, Sens. Actuators B 97 (2004) 387–390.

24. H.U. Lee, S.C. Lee, S. Choi, B. Son, H. Kim, S.M. Lee, H.J. Kim, J. Lee, Influence of visible-light irradiation on physicochemical and photocatalytic properties of nitrogen-doped three-dimensional (3D) titanium dioxide, J. Hazard. Mater. 258 (2013) 10–18.

25. Y.-D. Wang, Z.-X. Chen, Y.-F. Li, X.-H. Wu, Electrical and gas sensing properties of WO_3 semiconductor material, Solid-State Electron., 45 (2001) 639-644.

26. J. Zeng, M. Hu, W. Wang, H. Chen, Y. Qin, NO_2-sensing properties of porous WO_3 gas sensor based on anodized sputtered tungsten thin film, Sens. Actuators B 161 (2012) 447–452.

27. Z. Hua, M. Yuasa, T. Kida, N. Yamazoe, K. Shimanoe, High sensitive gas sensor based on Pd-loaded WO_3 nanolamellae, Thin Solid Films 548 (2013) 677–682.

28. F. Annanouch, S. Vallejos, C. Blackman, X. Correig, E. Llobet, CO and H_2 sensing with CVD-grown tungsten oxide nanoneedles decorated with Au, Pt or Cu nanoparticles, Procedia Eng. 47 (2012) 904–907.

29. R. Ionescu, A. Hoel, C.G. Granqvist, E. Llobet, P. Heszler, Low-level detection of ethanol and H_2S with temperature-modulated WO_3 nanoparticle gas sensors, Sens. Actuators B 104 (2005) 132–139.

30. S. Vallejos, P. Umek, T. Stoycheva, F. Annanouch, E. Llobet, X. Correig, P. De Marco, C. Bittencourt, C. Blackman, Single-step deposition of Au- and Pt-nanoparticle-functionalized tungsten oxide nanoneedles synthesized via aerosol-assisted CVD, and used for fabrication of selective gas microsensor arrays, Adv. Funct. Mater. 23 (2013) 1313–1322.

31. W. Zeng, C. Dong, B. Miao, H. Zhang, S. Xu, X. Ding, S. Hussain, Preparation, characterization and gas sensing properties of sub-micron porous WO_3 spheres, Mater. Lett. 117 (2014) 41–44.

32. T5F Technical Data Sheet, Seoul Optodevice, rev0.0, April 2010, www.socled.com.

33. OSV4YL5451B Data Sheet, OptoSupply, LED & Application Technologies, ver.A.2.

34. Y. Shigesato, Photochromic properties of amorphous WO_3 films, Jpn. J. Appl. Phys. 30 (1991) 1457–1462.

35. Z.D. Meng, L. Zhu, J.G. Choi, C.Y. Park, W.C. Oh, Preparation, characterization and photocatalytic behavior of WO_3-fullerene/TiO_2 catalysts under visible light, Nanoscale Res. Lett. 6 (2011) 1–11.

36. J.D. Vincent, J. Vampola, G. Pierce, M. Stegall, S. Hodges, Fundamentals of Infrared and Visible Detector Operation and Testing, Wiley and Sons, 2015.

37. A. Giberti, C. Malagù, V. Guidi, WO_3 sensing properties enhanced by UV illumination: An evidence of surface effect, Sens. Actuators B 165 (2012) 59–61.

38. Y. Shigesato, Photochromic properties of amorphous WO_3 films, Jpn. J. Appl. Phys. 30 (1991) 1457–1462.

38. K. Aguir, C. Lemire, D.B.B. Lollman, Electrical properties of reactively sputtered WO_3 thin films as ozone gas sensor, Sens. Actuators B 84 (2002) 1–5.

Tables

Table 1. Parameters of UV LEDs operated at a DC current of 20 mA.

	LED1	**LED2**
Peak wavelength [nm]	362	394
Optical power output [mW]	1.75	5
Forward voltage [V]	3.9	3.4
Spectrum half width [nm]	18	10
View angle [deg]	130	55/30

Table 2. Parameters of gas sensors exposed to synthetic air with 75 ppm of ethanol or methane, and 15 ppm of formaldehyde.

Ambient gas	C_2H_5OH	CH_4	CH_2O
Sensor operating temperature [°C]	200	200	200
LED1 DC current [mA]	8.3	8.3	8.3
LED2 DC current [mA]	10	10	10
Sensor DC current [μA]	12.5	12.5*	12.5
Sampling frequency [Hz]	2000	4000	2000
Number of recorded samples	348 000	1 024 000	348 000
Gas flow [ml/min]	133	100	100
Volume of the gas chamber [dm^3]	1.0	1.0	1.0

*2.66 μA during measurements without UV-light

Captions to the figures

Fig. 1. Gas sensor based on AuNP-decorated WO_3-NWs irradiated by use of UV diodes: 1 – wires for connection to preamplifier input and DC bias current, 2 – UV diode, 3 – sensor with a heater on the bottom side, 4 – mounting plate.

Fig. 2. Optical power spectra of light emitted by UV diodes, specifically LED1 (T5F) and LED2 (OSV4YL5451B). I_F denotes DC current.

Fig. 3. Relative changes of the DC resistance R_S of a gas sensor based on AuNP-decorated WO_3-NWs in the absence and presence of UV irradiation at 394 nm and upon repeated exposures to synthetic air (SA) and (a) 75 ppm of ethanol in SA and (b) 75 ppm of methane in SA. R_0 denotes DC resistance observed at the beginning of the measurements.

Fig. 4. Relative changes of the DC resistance R_S of a gas sensor based on AuNP-decorated WO_3-NWs in the absence and presence of UV irradiation at the shown wavelengths and upon exposure to synthetic air (SA) and to various concentrations of ethanol in SA. R_0 denotes DC resistance observed at the beginning of the measurements without UV-light (247 kΩ), with turned-on LED1 (161 kΩ) and with turned-on LED2 (52 kΩ).

Fig. 5. Normalized product of frequency f and power spectral density $S(f)$ of voltage fluctuations across a gas sensor based on AuNP-decorated WO_3-NWs, divided by the square of the bias voltage U_S and shown as a function of f. Data were recorded for the shown concentrations of ethanol in synthetic air in the absence (a) and presence of UV irradiation at the shown wavelengths (b) and (c).

Fig. 6. Relative changes of the DC resistance R_S of a gas sensor based on AuNP-decorated WO_3-NWs in the absence and presence of UV irradiation at the shown wavelengths and upon exposure to synthetic air (SA) and various concentrations of methane in SA. R_0 denotes the DC resistance observed at exposure to SA without UV-light (283 kΩ), with turned-on LED1 (176 kΩ) and with turned-on LED2 (63 kΩ).

Fig. 7. Normalized product of frequency f and power spectral density $S(f)$ of voltage fluctuations across a gas sensor based on AuNP-decorated WO_3-NWs, divided by the square of the bias voltage U_S and shown as a function of f. Data were recorded for the shown concentrations of methane in synthetic air in the absence (a) and presence of UV irradiation at the shown wavelengths (b) and (c).

Fig. 8. Relative changes of the DC resistance RS of a gas sensor based on AuNP-decorated WO_3-NWs in the absence and presence of UV irradiation at the shown wavelengths and upon exposure to synthetic air (SA) and to various concentrations of formaldehyde in SA. R_0 denotes DC resistance observed at exposure to SA without UV-light (103 kΩ), with turned-on LED1 (99.6 kΩ) and with turned-on LED2 (94.7 kΩ).

Fig. 9. Normalized product of frequency f and power spectral density $S(f)$ of voltage fluctuations across a gas sensor based on AuNP-decorated WO_3-NWs, divided by the square of the bias voltage U_S and shown as a function of f. Data were recorded for the shown concentrations of formaldehyde in synthetic air in the absence (a) and presence of UV irradiation at the shown wavelengths (b) and (c).

Figures

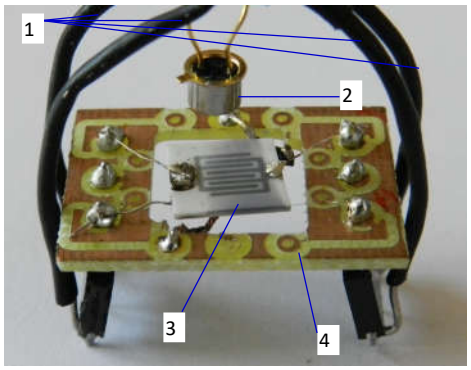

Figure 1.

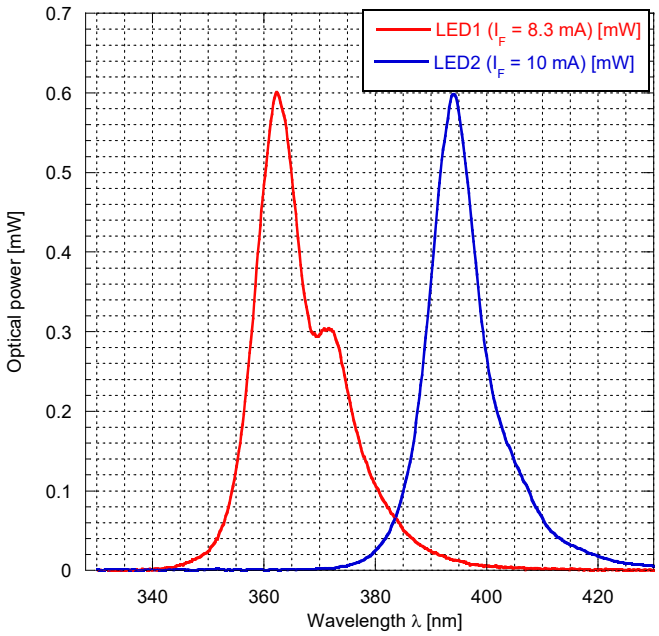

Figure 2.

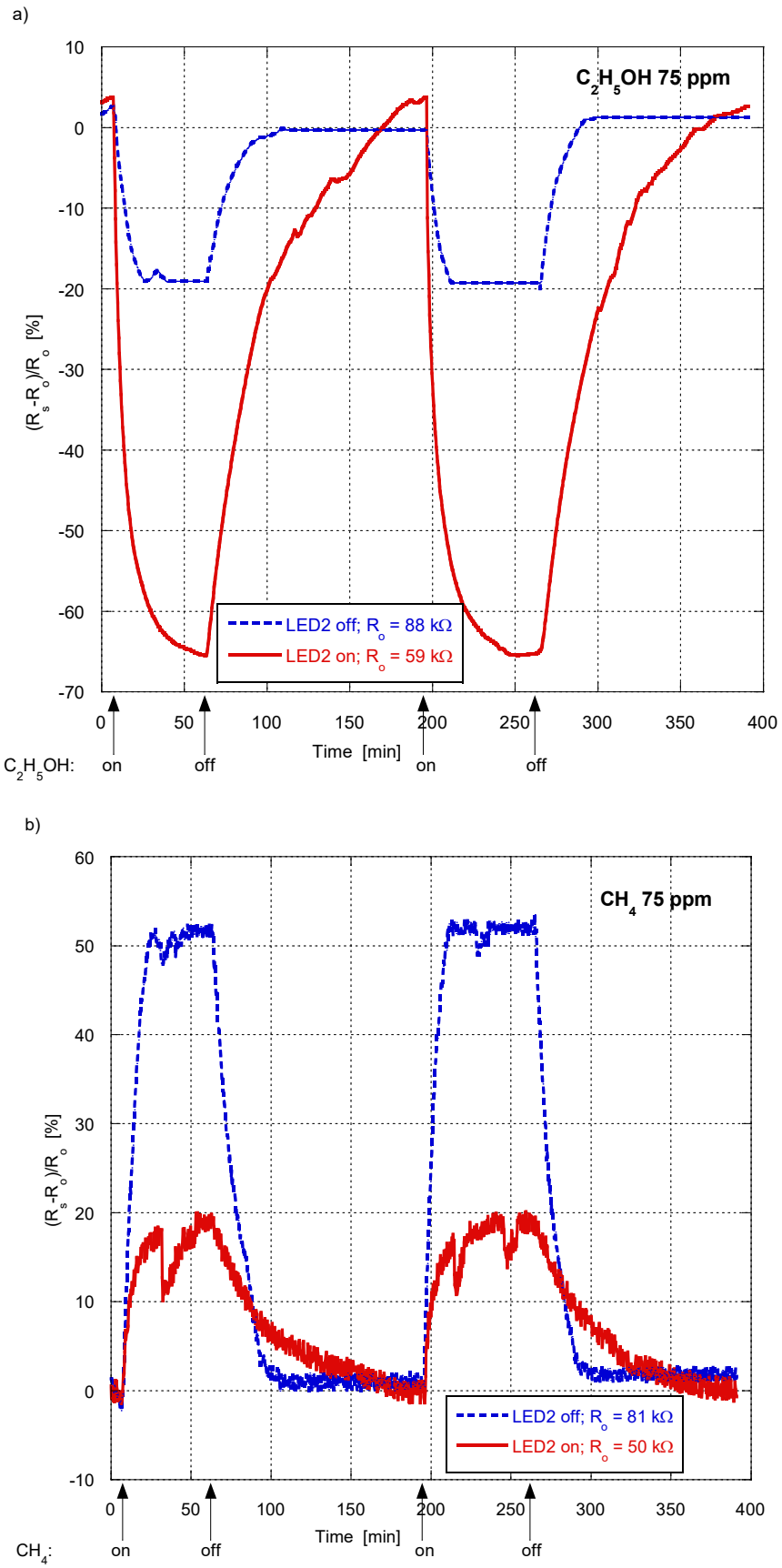

Figure 3.

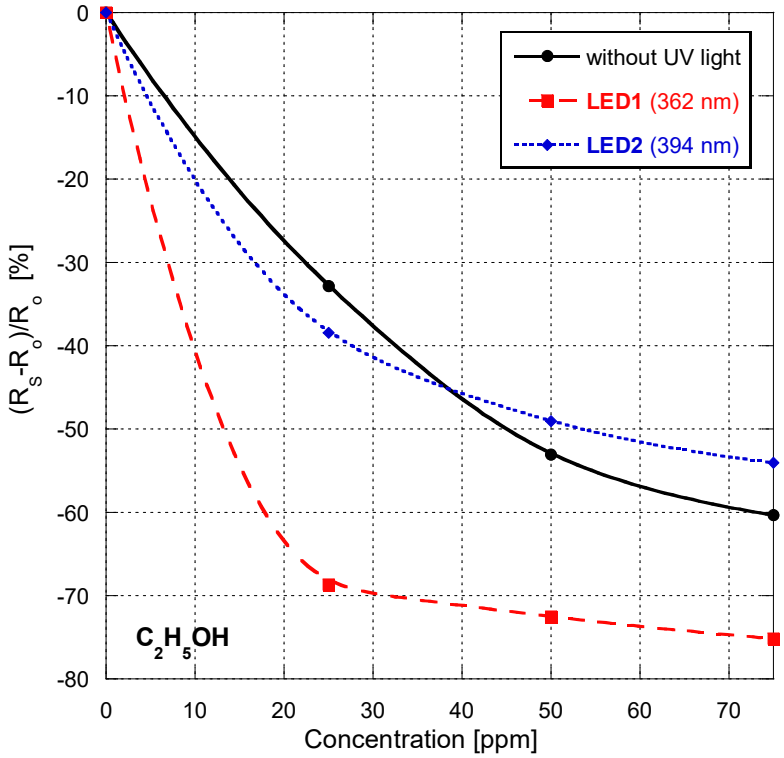

Figure 4.

a)

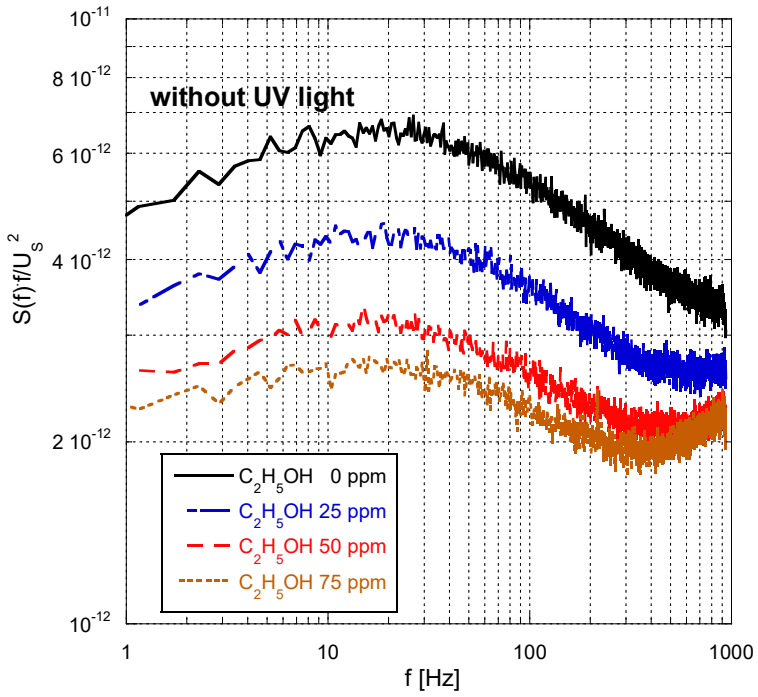

b)

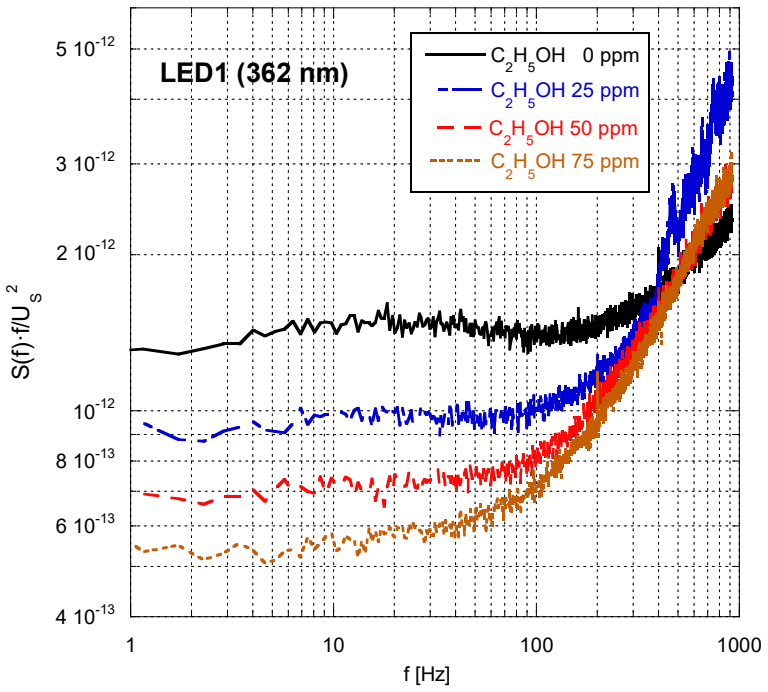

c)

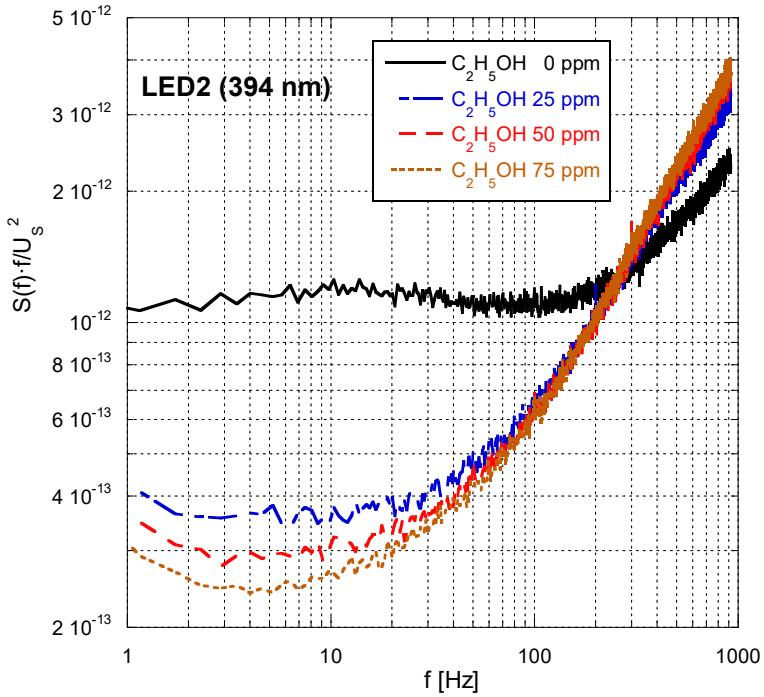

Figure 5.

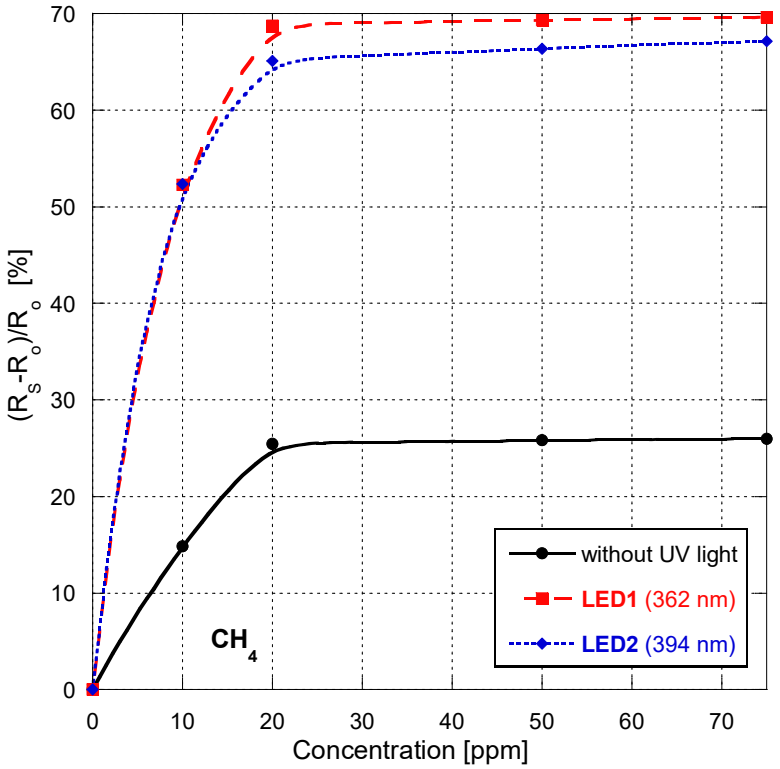

Figure 6.

a)

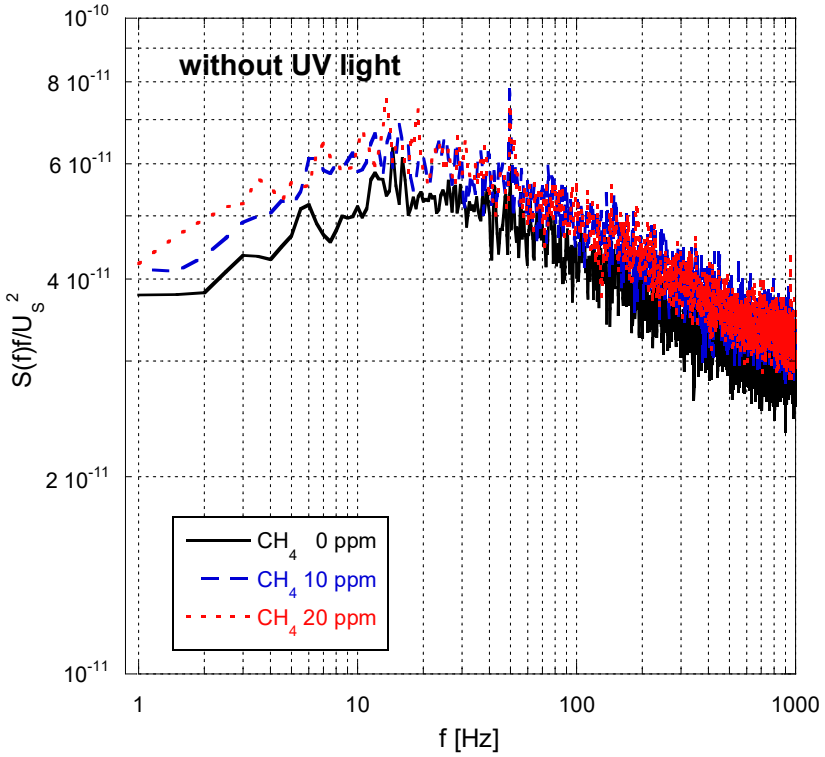

b)

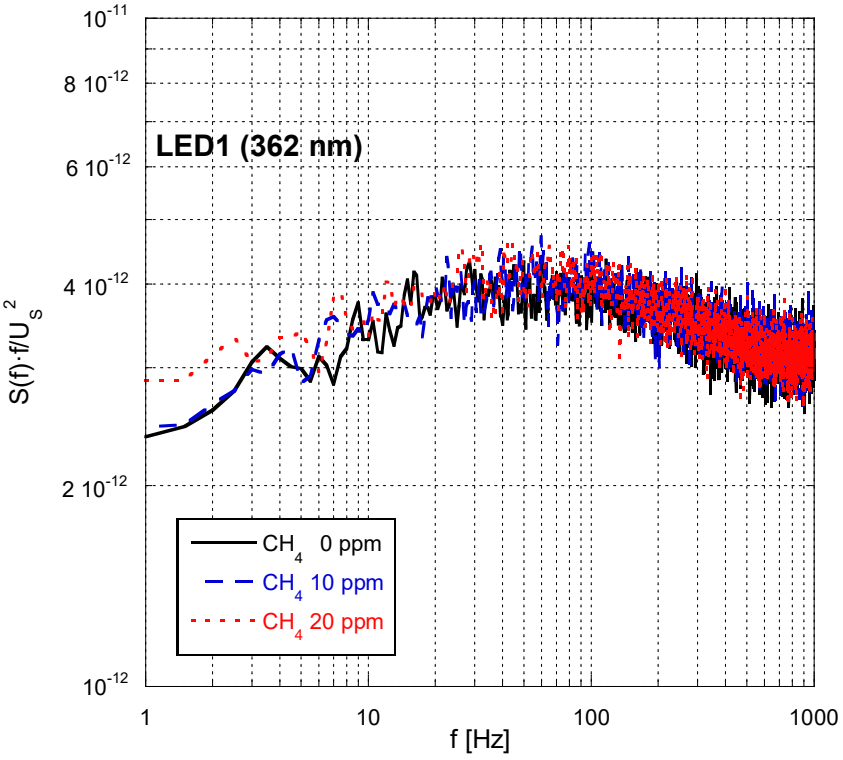

c)

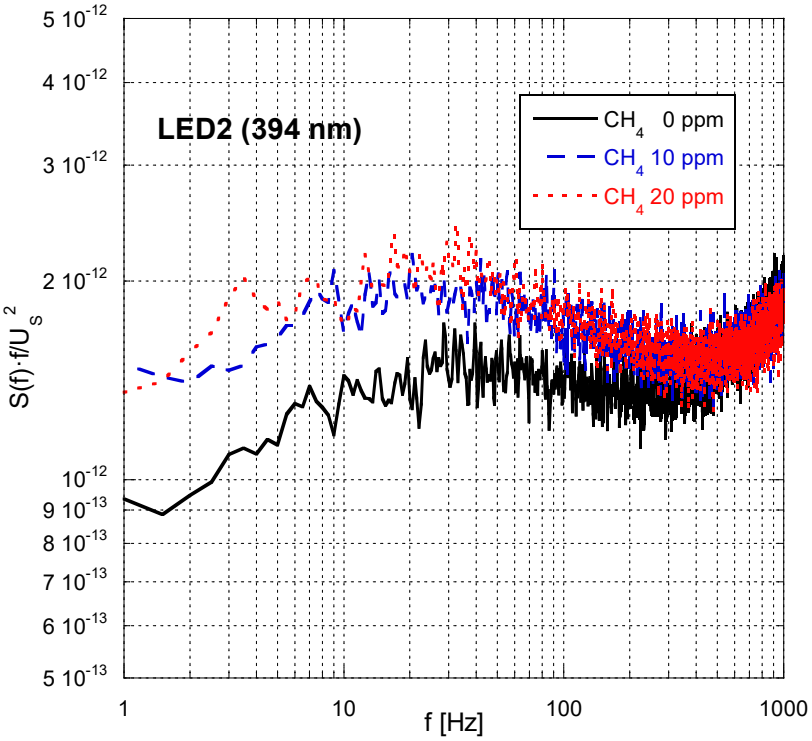

Figure 7.

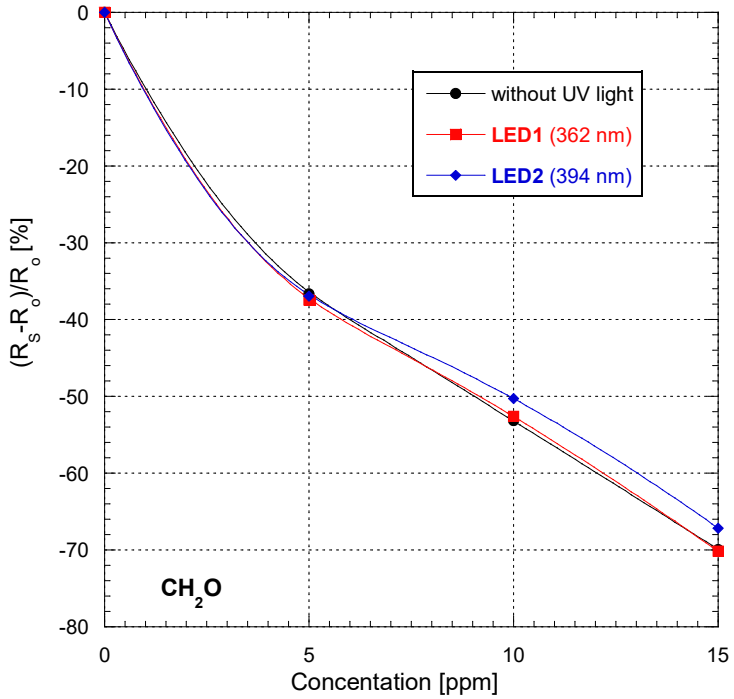

Figure 8.

a)

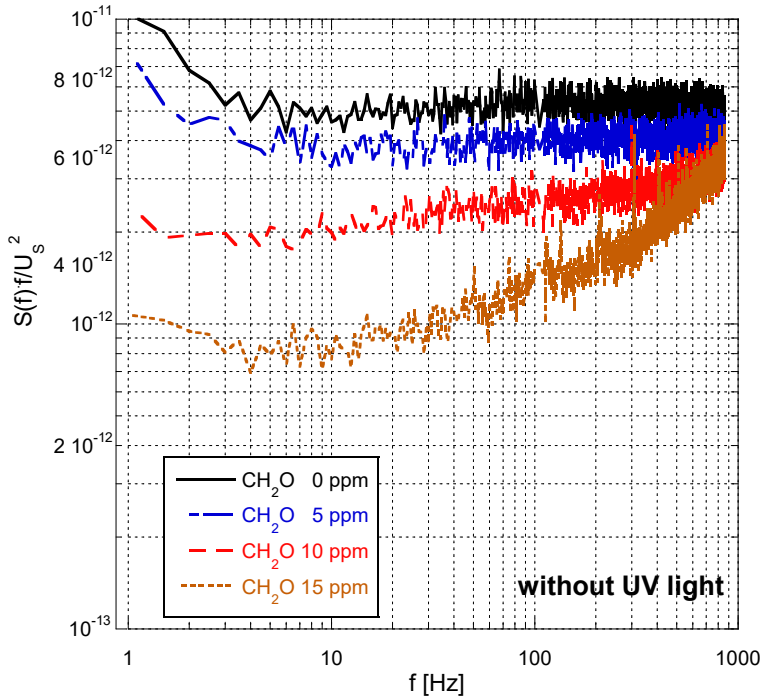

b)

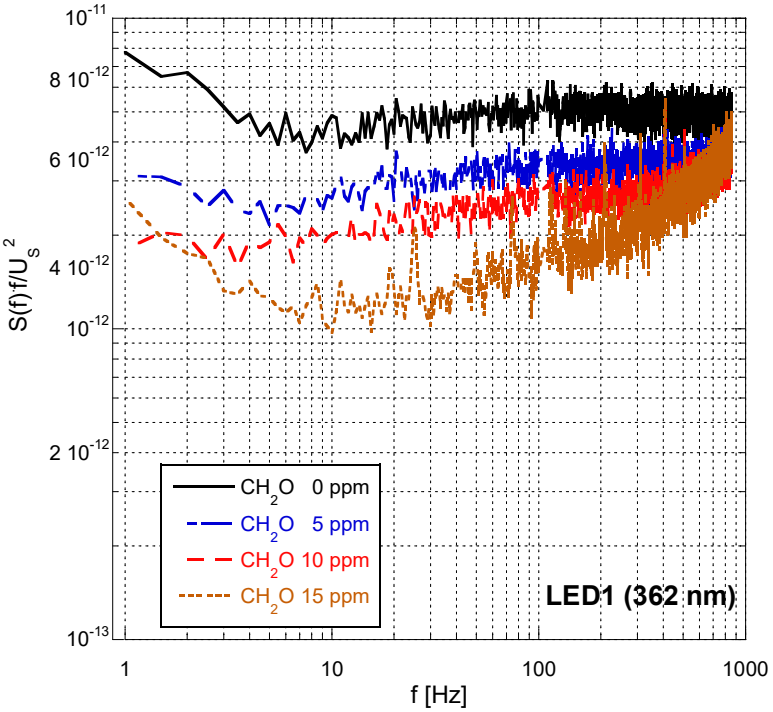

c)

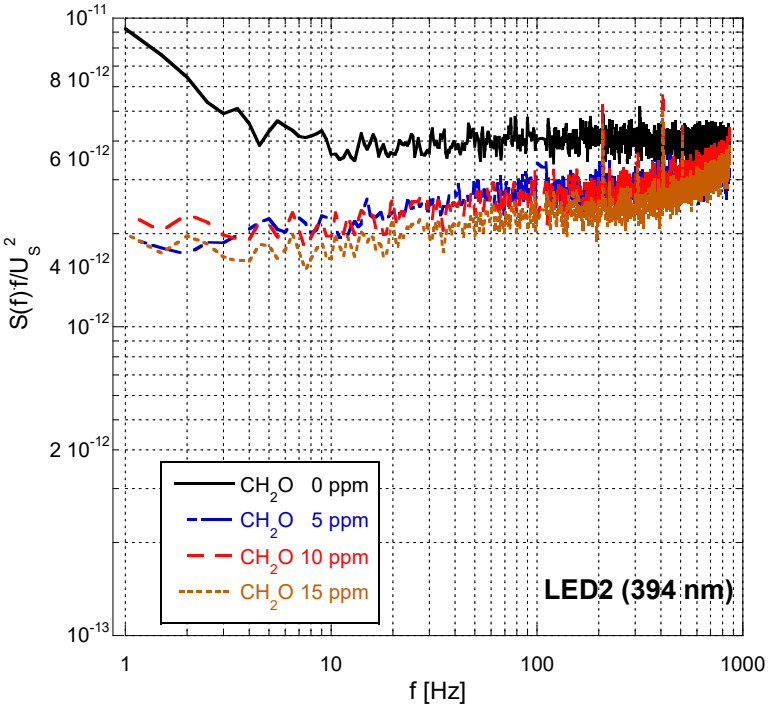

Figure 9.